Dicle University
Journal of Engineering
https://dergipark.org.tr/tr/pub/dumf
duje.dicle.edu.tr

Research Article

EEG-Based Comparative Study of Brain Activity during Imagined Natural and Induced Water and Saliva Swallowing

Sevgi GÖKÇE ASLAN[1*]

[1] Inonu University, Biomedical Engineering Department, sevgigokce38@gmail.com, Orcid No: 0000-0001-9425-1916

ARTICLE INFO

Article history:

Received 13 April 2025
Received in revised form 23 June 2025
Accepted 6 August 2025
Available online 30 September 2025

Keywords:

EEG, Dysphagia, Swallowing, Imagination, Statistical Analysis

Doi: 10.24012/dumf.1675408

* Corresponding author

ABSTRACT

Dysphagia often makes eating and drinking painful, stressful, and socially isolating, potentially leading to malnutrition, dehydration, weight loss, and respiratory infections. In this study, the relationship between swallowing and brain signals was examined to contribute to the electrophysiological understanding of the imagination of swallowing and rehabilitation of dysphagia patients. To examine the swallowing event, three different experiments were conducted. The experiments included (i) natural water swallowing, (ii) swallowing saliva in an induced manner, and (iii) swallowing a sip of water in an induced manner. Visual cues on a computer monitor were used to induce the perception of swallowing and imagination. EEG data from 16 channels obtained during 15 trials of these experimental paradigms from 30 subjects (15 men) were subjected to different processes such as noise removal, selection of signal segments corresponding to the imagination of swallowing, extraction of frequency domain features, and statistical analysis. Eleven features such as spectral centroid, mean and median frequency, delta, theta, alpha and beta band powers, and relative band powers obtained from 16 channels (a total of 176 features) were first subjected to the Shapiro-Wilks normality test individually. As a result of this test, the statistical analyses were carried out with the help of repeated measures one-way ANOVA test for the features with normal distribution (spectral centroid from 11 channels), and the Friedman test for the features with non-normal distribution (spectral centroid from the remaining 5 channels and all other features from 16 channels). As a result of these tests, it is seen that 76.7% of all features yield statistically significant differences between 3 different swallowing approaches. We suggest that identifying discriminative EEG-based features could significantly contribute to the development of novel brain-machine interface applications for dysphagia rehabilitation.

1. Introduction

Swallowing is a fundamental physiological function essential for nutrition and hydration. However, for individuals with dysphagia, this simple act becomes a daily challenge, leading to significant physiological, psychological, and social difficulties [1]. Although dysphagia itself is not immediately life-threatening if left untreated, it can result in severe complications such as malnutrition, dehydration, and pneumonia due to impaired swallowing function [2], [3], [4]. Therefore, early and accurate diagnosis is crucial to improving patients' quality of life and preventing potentially life-threatening consequences.

Conventional methods, such as nasopharyngeal endoscopy and video fluoroscopy, are commonly used to assess swallowing function [5], [6]. While effective, these techniques can be invasive, uncomfortable, and require specialized clinical settings. As a result, there is an increasing demand for non-invasive and accessible alternatives for dysphagia detection and monitoring. Recent research highlights brain activity analysis as a promising approach for identifying swallowing-related impairments without direct intervention.

Among these methods, EEG stands out due to its non-invasiveness, high temporal resolution, affordability, and ease of application in clinical settings [7]. EEG records electrical brain activity through scalp electrodes, capturing voltage fluctuations associated with neuronal activity. Modern EEG systems can detect signals exceeding 1 kHz, enabling the recording of rapid neural changes critical for analyzing phenomena like epileptiform spike waves [8], [9], [10], [11] .

EEG has been used to diagnose various neurological and psychiatric disorders, including schizophrenia, Alzheimer's disease, depression, and epilepsy [12], [13], [14], [15]. In recent years, significant progress has also been made in utilizing EEG to analyze brain activity related to motor control [16]. In particular, motor imagery (MI) has emerged as a valuable paradigm for exploring cortical mechanisms involved in voluntary movement and for developing brain-computer interface (BCI) applications in neurorehabilitation [17].

Within the domain of swallowing research, MI has been effectively used to examine the cortical dynamics underlying swallowing control and to design EEG-based BCI systems for dysphagia rehabilitation [18]. In addition to these recent advancements, earlier foundational studies have offered critical insights into the neural basis of swallowing [19]. Yang et al. proposed that swallowing is initiated by tongue movement and suggested that gaps in

brain activity could indicate the absence of swallowing initiation[20], [21]. Jestrovic et al. explored how distractions influence brain activity during swallowing [22], while Huckabee et al. investigated the role of the cerebral cortex in motor planning and initiation of swallowing [23].

Building upon these developments, a recent systematic review by Alexandropoulou et al. emphasized that EEG-based studies on swallowing have increasingly revealed the cortical involvement not only during the preparatory but also during pharyngeal and esophageal phases of swallowing, challenging the earlier notion of these phases as purely reflexive. The review also highlighted using motor imagery (MI) paradigms in eliciting movement-related cortical potentials (MRCPs), mu rhythm desynchronization, and distinct connectivity patterns within sensorimotor networks. Moreover, swallowing-related EEG activity is modulated by factors such as stimulus type, bolus volume, and task complexity, and exhibits non-stationary dynamics and lateralized activation, which are relevant for developing brain-computer interfaces for dysphagia rehabilitation [24].

However, many previous studies have focused either on spontaneous swallowing or single-task MI protocols without clearly distinguishing among different imagined swallowing types, such as natural vs. induced swallowing or saliva vs. water. Furthermore, most existing EEG studies have been limited to narrow feature sets or few electrode sites, lacking comprehensive multichannel frequency-domain analysis.

In contrast to prior work limited to spontaneous or distraction-based swallowing tasks, this study aims to explore the relationship between brain function and swallowing through multichannel EEG recordings using controlled experimental paradigms. Specifically, swallowing was examined under three distinct conditions: natural water swallowing, induced water swallowing, and saliva swallowing. The study involved thirty right-handed participants of varying ages, all of whom had no history of neurological disorders or speech and swallowing impairments. EEG signals recorded from 16 channels underwent preprocessing, noise reduction, selection of swallowing imagination segments, and frequency-domain feature extraction before statistical analysis. We hypothesize that imagining swallowing water and saliva under different conditions exhibits distinct electrophysiological characteristics. Identifying discriminative EEG-based features may contribute to the development of novel brain-machine interface applications for dysphagia rehabilitation, offering a non-invasive and effective alternative for clinical assessment and treatment.

2. Materials And Methods

2.1 Participants

Our experiments were conducted with 30 participants (15 men and 15 women) aged between 19 and 56, with an average age of 30 and a standard deviation of 12. All participants were free from any swallowing disorders or related medical conditions. The study utilized three experimental paradigms approved by the Erciyes University Ethics Committee on July 12, 2023, under approval number 2023/461.

2.2 Materials

In our experiments, we utilized a 16-channel Nautilus research-grade wearable EEG headset (g.tec medical engineering, Schiedlberg, Austria) to acquire EEG signals (Figure 1). Due to its wearable design, the headset with dry electrodes was comfortably fitted onto the participant's head. The EEG electrodes were positioned following the International 10-20 system, and the signals were recorded at a sampling frequency of 500 Hz. The electrode placements on the participants' skulls are illustrated in Figure 2. EEG data were collected within 0.5–200 Hz. range using MATLAB Simulink on a Windows operating system.

Figure 1. Nautilus research-grade wearable EEG headset.

2.3 Experimental Procedure

In this study, no additional devices or sensors were attached to the neck or other body parts to detect swallowing; all analyses were conducted solely using EEG signals. To examine brain activity associated with swallowing, we not only focused on the swallowing process itself but also incorporated conditions that could potentially influence neural activity, such as pre-swallowing rest and imagined swallowing, into our experimental protocols. Consequently, our analyses were carried out across three distinct experimental conditions.

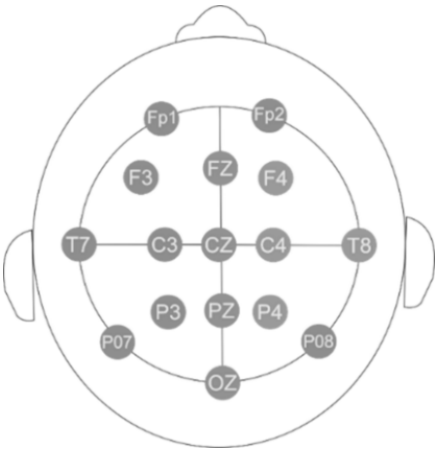

Figure 2. International 10-20 electrode placement system.

2.3.1 Paradigm 1: Natural Water Swallowing

Our first experimental paradigm aimed to examine the EEG signals of the spontaneous and natural imagination state in the brain before swallowing, without giving the subject an imagined swallowing warning (no induced swallowing). The subject was seated in front of the computer for the experiment, and the EEG electrodes were placed over the subject's skull. The subject was given a bottle of water and a straw and asked to follow the warnings/cues that appeared on the screen at regular intervals to draw a sip of water from the bottle and drink. This experiment started with the beep sound, and 2 seconds after the beep sound, the water inscription appeared on the screen for 5 seconds, and the subject drank the water in the bottle using a straw in his/her mouth during this time without any further visual cue, with minimal or no movement. Then, the subject was asked not to perform any activity for 3 seconds. This experiment consisted of 15 trials and took 150 seconds in total. The graphic showing a trace of our first experiment, which we call natural swallowing, can be seen in Figure 3.

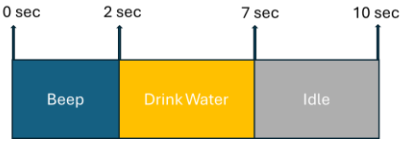

Figure 3. Natural swallowing test procedure with corresponding timing information.

2.3.2 Paradigm 2: Induced Saliva Swallowing

In contrast to the first paradigm, this experiment required participants to first rest, then imagine swallowing, and finally swallow without consuming any food or liquid. Referred to as the saliva swallowing experiment, its objective was to examine the effects of swallowing without ingestion on EEG signals. The experiment consisted of three phases: resting, imagination, and swallowing. During the resting phase, participants focused on a plus symbol displayed on the screen for 2 seconds. Following this, a beep sound signaled the start of the imagination phase, where participants envisioned swallowing for 3 seconds while viewing the prompt "imagination." In the final stage, the word "swallow" appeared on the screen, prompting participants to perform actual saliva swallowing. Each trial in this experiment lasted 9 seconds, with 15 trials totaling 135 seconds. Figure 4 illustrates a graphical representation of a 9-second segment of the dry swallowing test.

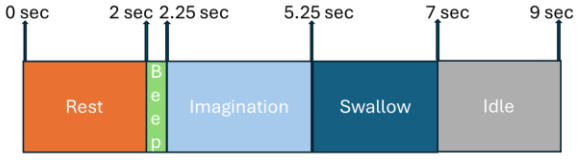

Figure 4. Saliva swallowing test procedure with corresponding timing information.

2.3.3 Paradigm 3: Induced Water Swallowing

In our final experimental paradigm, referred to as induced water swallowing, we aimed to investigate the impact of imagining the act of swallowing a sip of water held in the mouth on EEG signals. This experiment comprised four stages: water intake, resting, imagination, and actual swallowing. Participants were provided with a bottle of water and a straw and instructed to follow the cues displayed on the screen. Unlike the previous experiments, this paradigm involved the presence of water in the mouth during the imagination phase.

In the first stage, upon seeing the cue "draw water" on the screen, participants took a sip of water using the straw. Next, a plus symbol appeared for 2 seconds, during which participants engaged in the resting phase by focusing on the symbol. In the third stage, the screen displayed the word "imagination," prompting participants to mentally simulate swallowing the water for 3 seconds. Finally, in the last stage, they were instructed to perform an actual swallow. Each trial lasted 13 seconds, with a total of 15 trials, amounting to 195 seconds. Figure 5 illustrates a 13-second segment of this experiment.

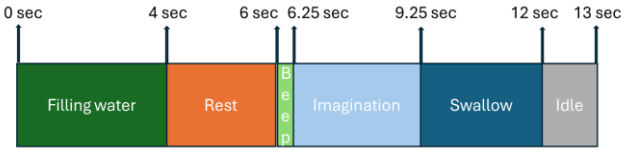

Figure 5. Water swallowing test procedure with corresponding timing information.

3. Data Analysis

3.1 Filtering

First, we performed denoising on the EEG data obtained from each subject since swallowing may cause different artifacts. We filtered EEG signals with a bandpass filter in the range of 2-30 Hz to remove low-frequency motion artifacts and high-frequency muscle artifacts. The 2–30 Hz band was selected to minimize the effects of swallowing-related artifacts. Swallowing-induced movement artifacts typically dominate frequencies below 2 Hz due to head and neck motions, while muscle activity artifacts often affect frequencies above 30 Hz. Therefore, this bandpass range was chosen to retain cortical activity while suppressing peripheral noise.

Artifact removal was performed using Independent Component Analysis (ICA), implemented via the FastICA algorithm with the 'gauss' nonlinearity function, where the number of independent components was set equal to the number of EEG channels. After ICA decomposition, each independent component (IC) was subjected to Continuous Wavelet Transform (CWT) analysis to detect abrupt high-frequency fluctuations (spikes) associated with ocular and muscle artifacts (e.g., eye blinks, facial movements). Peaks identified on CWT coefficient curves were used to automatically mark artifact-contaminated time intervals. These segments were suppressed (set to zero), and the cleaned EEG signals were reconstructed by recombining the remaining ICs through the mixing matrix A.

As a result of these processes, we have cleaned our EEG signals from artifacts. An example of filtered and unfiltered EEG signals can be seen in Figure 6.

The signal shown in Figure 6a represents a one-channel raw EEG signal (Channel 13) from one subject during 15 trials of an induced saliva swallow experiment. Figure 6b shows the filtered version of the same signal depicted in Figure 6a.

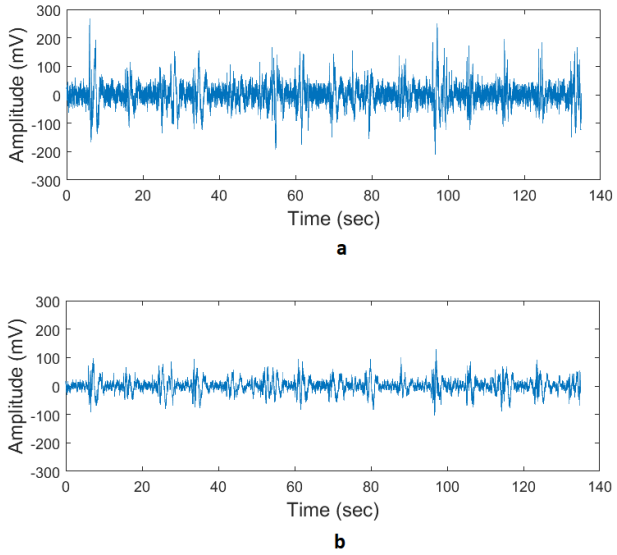

Figure 6. a) Raw signal and b) filtered signal after bandpass filtering and ICA.

3.2 Selection of Signal Segments Corresponding to Imagination

In our first experiment, natural water swallowing, the subjects were not shown any imagination-related commands and were not given specific imagination onset time information. In the natural water swallowing experiment, we aimed to analyze our data regarding how subjects imagine spontaneous swallowing before the actual swallowing movement. Since each subject's swallowing onset and finishing time instants differed from each other while performing the experiments, we examined the EEG signals from 30 people individually. Considering that each person's reaction time to actions was different in each trial, we decided to manually determine the dynamic onset time for swallowing using the motion and muscle artifacts on the EEG signals. Each person had different pre-swallow times in each trial. We considered the signal segments from our individually analyzed signals to the actual swallowing onset time manually as the imagination segment. We selected and recorded the part of the imagination that we determined from our EEG signals. We thought that the signal values with an imagination time of less than 0.5 seconds did not represent a valid signal for the Fourier analysis, which we have employed in the feature selection part of the study. Therefore, we did not include the trials whose imagination durations were less than 0.5 seconds for further analysis. Figure 7 shows the signals from different channels and different trials of 4 different subjects acquired during the natural water swallowing experiment. We included the signals shown in Figures 7a, b, and c, but not d, which had an imagination duration of less than 0.5 seconds. After this selection and elimination process, we were left with 190 trials and 3040 (190x16, number of trials x number of channels) imagination segments.

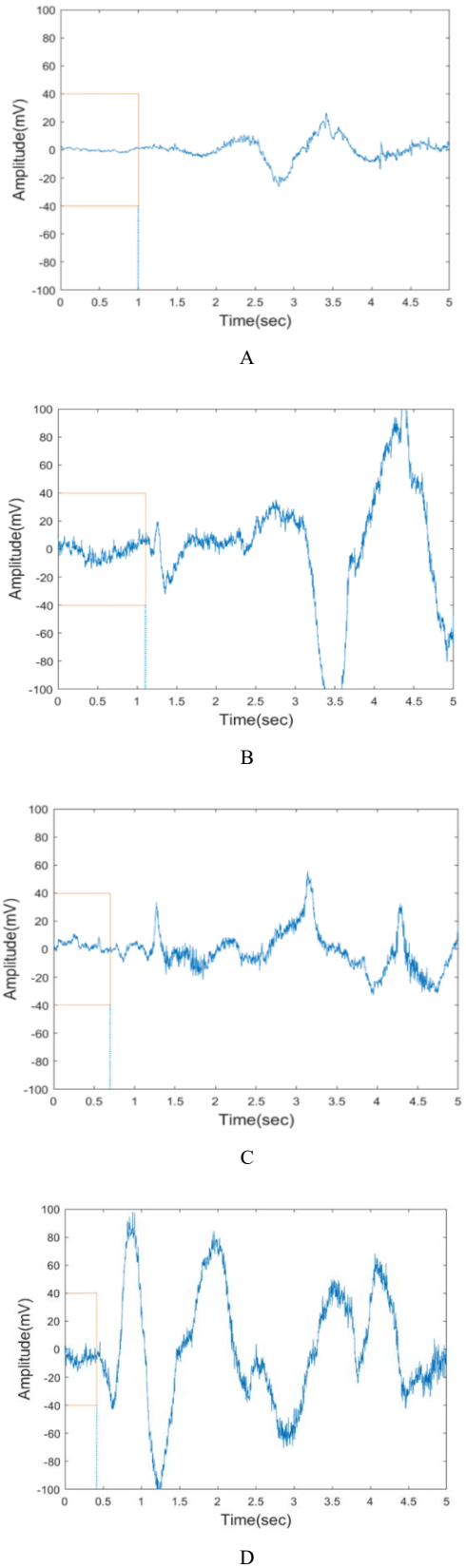

Figure 7. The selected segments corresponding to the imagination process from 4 different subjects, from different channels, and trials. Imagination durations were 1 second in (A), 1.2 seconds in (B), 0.6 seconds in (C), and 0.4 seconds in (D).

In the other two experiments, induced saliva and induced water swallowing experiments, the subjects were shown the visual cue on the screen to initiate and end the imagination of swallowing, unlike the first experiment. The imagination segments of these two experiments, of which we were certain about the imagination onset and finishing time instants, were selected and recorded. After this selection process, we obtained 450 trials and 7200 imagination segments (30 subjects x 15 trials x 16 channels).

Finally, for a consistent comparison and statistical analysis, if the imagination segments from a trial obtained during a natural water swallowing experiment for a subject were eliminated due to short signal duration, we eliminated the segments from the same trial number obtained during induced saliva and induced water swallowing experiments for the same subject. Therefore, 190 trials and 3040 imagination segments were also left for the induced saliva and induced water swallowing experimental paradigms individually.

3.3 Feature Extraction

We extracted the features from the EEG signals corresponding to the imagination of different swallowing approaches/paradigms. The feature extraction approach was based on the frequency domain. The frequency-domain features were mean frequency (in the power spectrum), median frequency (in the power spectrum), spectral centroid, band power in the delta band, band power in the theta band, band power in the alpha band, band power in the beta band, relative power in delta band, relative power in the theta band, relative power in the alpha band, and relative power in the beta band.

The mean frequency of a spectrum is calculated using Equation (1). In this equation, n is the number of frequency bins in the spectrum, f_i is the spectrum frequency in the ith bin, and I_i represents the intensity of the spectrum (in dB scale) in the ith bin.

$$f_{mean} = \frac{\sum_{i=0}^{n} I_i \cdot f_i}{\sum_{i=0}^{n} I_i} \quad (1)$$

The median frequency of a spectrum is calculated in two steps. First, the intensity in the signal across the entire spectrum is summed and divided by two. Next, a frequency is chosen where the cumulative intensity (i.e., all intensity values for lower frequencies, including focal intensity) exceeds the value calculated in the first step for the first time.

The spectral centroid is a measure used to characterize a spectrum and indicates where the center of mass of the spectrum is. As shown in equation (2), mi represents the magnitude of the bin number, and fi represents the center frequency of the bin.

$$\mu = \frac{\sum_{i=1}^{N} f_i \cdot m_i}{\sum_{i=1}^{N} m_i} \quad (2)$$

Powers in delta (0-3.9 Hz), theta (3.9-7.8 Hz), alpha (7.8-15.63 Hz), and beta (15.63-31.25 Hz) bands were calculated using a 6-level decomposition of the discrete wavelet transform. The relative power of bands was derived using the power values in each band divided by the power summed over these frequency bands. To obtain a percentage, we multiplied the ratios by 100. Thus, the relative power values were computed using the ratio of a specific band power to the total spectral power in the signal under consideration.

We extracted these 11 features in the frequency domain for 16 channels for each imagination segment. Therefore, for each segment, we obtained a total of 176 features (11 x 16).

3.4 Statistical Tests

The aim of the final stage of this research was to investigate which of these features were significantly different from each other in these different experiments using appropriate statistical tests. For values with a p-value greater than 0.05, the difference between groups is considered not significant. p-values less than 0.05 are categorized as significant, p-values less than 0.01 as very significant, and p-values less than 0.001 as highly significant.

3.4.1 Normality Check for Features

It is possible to use various normality tests to reveal whether the feature we are interested in is suitable for a normal distribution. The most well-known tests are the Chi-Square, Kolmogorov-Smirnov, Lilliefors, and Shapiro-Wilk normality tests. We decided to use the Shapiro-Wilk test because it is the most powerful test of the normality assumption [25]. We conducted our experiments with less than 50 subjects. First of all, with the Shapiro-Wilk test, we determined which features have normal or non-normal distribution among 176 features. Then, we performed a parametric test (repeated measures one-way analysis of variance, ANOVA) for normally distributed variables and a non-parametric test (Friedman test) for variables that have non-normal distribution.

3.4.2 Analysis of Features with Normal Distribution

ANOVA is a tool used to test whether there is a statistically significant difference between the means of independent groups. Repeated measures ANOVA is the extension of the dependent t-test and is the counterpart of the one-way ANOVA, but for related groups. We used the repeated measures ANOVA test to analyze the features that had a normal distribution. As a result of this test, we were able to find the features that had statistical significance, including the level of significance (according to the p-value) between three swallowing approaches/paradigms.

3.4.3 Analysis of Features with Non-normal Distribution

The Friedman test is the non-parametric equivalent of the one-way repeated ANOVA test. The Friedman test is used if the data are not normally distributed, the number of groups/conditions is three or more, and the same subjects are used in all groups/conditions. We subjected features with non-normal distribution to the Friedman test and were able to find the features that had statistical significance

including the level of significance between three swallowing approaches/paradigms.

3.5 Classification

Classification analysis was performed using a set of 135 significant features selected from the original dataset. Feature matrices corresponding to the three classes were concatenated for each paradigm, and the resulting data were standardized using z-score normalization to ensure comparable scales across features.

To evaluate classification performance, both binary and multi-class tasks were considered. Specifically, class combinations included binary pairs (Paradigm 1 vs 2, Paradigm 2 vs 3, and Paradigm 1 vs 3) as well as a multi-class scenario involving all three paradigms simultaneously.

For each class combination, the relevant subset of data was extracted. In binary classification cases, class labels were relabeled as 1 and 2 for consistency. A 10-fold cross-validation strategy was employed to assess model generalizability and prevent overfitting.

Four different classifiers were evaluated: Random Forest, Support Vector Machine (SVM) with Radial Basis Function (RBF) kernel, K-Nearest Neighbors (KNN), and Decision Tree. To optimize classifier performance, a grid search was conducted over relevant hyperparameters for each model:

- Random Forest: Number of learning cycles (100, 200, 300) and maximum number of splits per tree (20, 50, 100).
- SVM: Kernel scale parameters ([0.1, 0.5, 1, 2, 5, 10]) for the RBF kernel.
- KNN: Number of neighbors ([3, 5, 7, 9]).
- Decision Tree: Maximum number of splits ([10, 20, 50]) and minimum leaf size ([1, 5, 10]) within an ensemble framework using 100 learning cycles.

During each fold of cross-validation, classifiers were trained on the training subset and evaluated on the test subset. The best accuracy across hyperparameter combinations was recorded per fold for each classifier. Final reported accuracies represent the average performance over all folds.

The combined use of cross-validation and hyperparameter tuning ensured robust and unbiased estimates of classification accuracy across different class combinations and models.

4. Results

As the outcome of the normality test, we determined that 11 of 176 features have a normal distribution, and the rest have a non-normal distribution. These 11 features were spectral centroid values from 11 channels. The remaining spectral centroid features from 5 channels and all other frequency domain features from 16 channels followed a non-normal distribution. Figure 8 shows the distribution of 4 sample features, 2 of which had normal distribution, and 2 of which had non-normal distribution.

When the spectral centroid features from 11 channels with normal distribution were subjected to a one-way repeated measures ANOVA test, 10 features were found to be very significant, and 1 value was found to be significant. In other words, this result means that all p-values were less than 0.05. This indicates that there is statistical significance between the three different paradigms for the imagination of swallowing in terms of spectral centroid features from 11 channels.

When we examined the features with non-normal distribution using the Friedman test, features such as mean frequency, median frequency, spectral centroid, delta band power, and beta band showed statistically significant differences between imagination paradigms in all 16 channels. On the contrary, a feature such as the power of the theta band showed non-significant differences in all channels. Features such as the power of the alpha band, the relative power of theta band, the relative power of the alpha band, and the relative power of the beta band showed significant and non-significant differences. Table 1 shows how many channels for each feature with a non-normal distribution have which level of statistical significance.

The p-values in the ANOVA and Friedman tests, which we applied for our features with normal and non-normal distributions, show that the group mean differences are not significant or significant. In these test results, 11 features with normal distribution and 124 with non-normal distribution seem statistically significant. We also performed multiple comparison tests to determine which groups were groups with different means for the 41 non-normally distributed and non-significant features. As a result of the test, we calculated the mean and standard deviation values between the groups. The comparison results of 41 non-significant features that we obtained are shown in Table 2. Although the features in Table 2 did not reach statistical significance, the observed trends in mean values across paradigms reveal subtle but potentially meaningful neural differences. These trends, particularly in frontal and parietal regions, suggest differentiated cortical engagement during various swallowing imagination conditions. Such latent patterns may contribute to classification success, highlighting the utility of multivariate approaches beyond univariate statistical thresholds.

The classification results for different class combinations using 135 significant features and various classifiers are summarized in Table 3. The binary classification tasks involving pairs of paradigms (Paradigm 1 vs 2, Paradigm 2 vs 3, and Paradigm 1 vs 3) consistently achieved higher accuracies compared to the multi-class classification involving all three paradigms simultaneously (Paradigms 1 vs 2 vs 3). Among the classifiers, Random Forest demonstrated the best overall performance, achieving the highest average accuracy in all binary tasks, with accuracies of 75.26%, 71.58%, and 76.58% for Paradigm 1 vs 2, Paradigm 2 vs 3, and Paradigm 1 vs 3 classifications, respectively. Similarly, Decision Tree showed competitive results, particularly in the Paradigm 1 vs 3 classification with an accuracy of 77.11%.

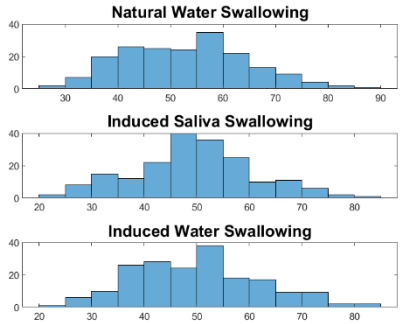

A

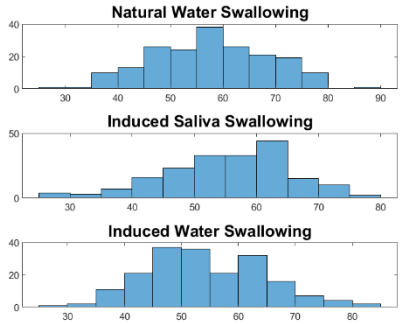

B

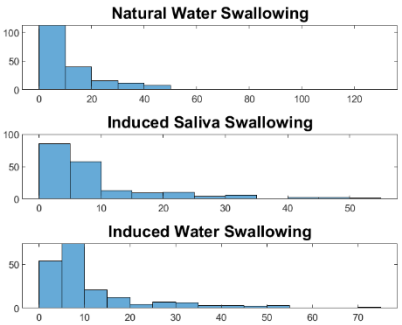

C

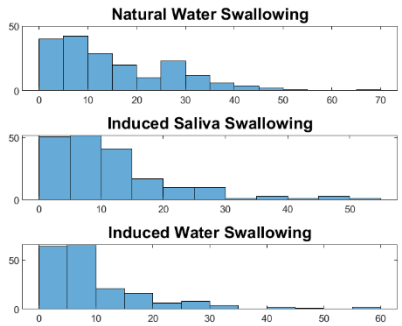

D

Figure 8. Histograms of two features with normal distributions (A and B) and two features with non-normal distributions (C and D). A) the Spectral centroid of channel 5, B) the spectral centroid of channel 15, C) the band power in the delta band of channel 11, and D) the mean frequency of channel 14.

The multi-class classification involving all three paradigms simultaneously yielded lower accuracy values across all classifiers, with the highest accuracy being 60.18% for Random Forest. This decrease is expected due to the increased complexity of distinguishing among three classes instead of two.

Support Vector Machine (SVM) with RBF kernel and K-Nearest Neighbors (KNN) classifiers showed moderate performance in all cases, with SVM slightly outperforming KNN in most tasks.

Overall, these results indicate that binary classification between pairs of paradigms is more reliable for this dataset, and ensemble methods like Random Forest are well-suited for the task. The reduced accuracy in multi-class classification suggests that further feature engineering or more advanced classification methods may be needed to improve performance when distinguishing among all three paradigms simultaneously.

5. Conclusions and Discussion

In this study, we tried to determine the relationship between swallowing and brain signals to contribute to the treatment of dysphagia patients with swallowing difficulties. While examining this relationship, we not only depended on the act of swallowing but also applied different paradigms before and after each experiment. We collected EEG signals of imagination of swallowing, waiting for swallowing, and actual swallowing events from 3 different experiments. By filtering each of the EEG signals from 16 channels in these experiments, we removed noise and unwanted components. In this article, we have focused specifically on the imagination states of the filtered signals. We extracted 176 features from the EEG signal segments corresponding to the imagination of swallowing. As a result of statistical analysis, we observed that 135 of 176 features (76.7%) revealed significant differences between the three experiments. We obtained these results from 30 subjects, clearly showing the relationship between the imagination of swallowing events and brain signals. One of the key novelties of this study is the integration of statistical analysis with machine learning, where significant features were used to classify the three swallowing paradigms with over 77% accuracy in binary settings.

To address dysphagia effectively, it is essential to examine swallowing from an electrophysiological perspective. Investigating electrophysiological processes enhances our understanding of swallowing control networks and provides a valuable tool for assessing the effects of various treatments on pharyngeal sensory function. In the literature, [26]. ERPs are signals derived from EEG recordings that measure time-dependent neural activity in response to sensory, motor, or cognitive events [27]. The swallowing process involves the neural transmission and cerebral integration of oropharyngeal sensory inputs, which can be investigated through ERP studies [26].

Table 1. Friedman test results for features with non-normal distribution. NS: Non-significant, S: Significant, HS: Highly Significant, VHS: Very Highly Significant.

Feature	NS	S	HS	VHS	Total
Mean Frequency				**16** Cz, Fp2, F3, Fz, F4, T7, C3, Fp1, C4, T8, P3, Pz, P4, Po7, Po8, Oz	**16**
Median Frequency				**16** Cz, Fp2, F3, Fz, F4, T7, C3, Fp1, C4, T8, P3, Pz, P4, Po7, Po8, Oz	**16**
Centroid Fft		**1** Oz	**2** Fp1, C4	**2** T8, P3	**5**
Power Delta		**4** Cz, Fz, F4, Oz	**11** Fp2, F3, T7, C3, Fp1, C4, T8, P3, Pz, P4, Po8	**1** Po7	**16**
Power Theta	**16**				**16**
Power Alpha	**5**	**5** Fz, C4, T8, P3, P4	**6** Fp2, F3, Pz, Po7, Po8, Oz		**16**
Power Beta				**16** Cz, Fp2, F3, Fz, F4, T7, C3, Fp1, C4, T8, P3, Pz, P4, Po7, Po8, Oz	**16**
Relative Power Delta		**1** Cz		**15** Fp2, F3, Fz, F4, T7, C3, Fp1, C4, T8, P3, Pz, P4, Po7, Po8, Oz	**16**
Relative Power Theta	**6**	**9** Cz, Fp2, F3, Fz, T7, C3, Fp1, C4, T8	**1** F4		**16**
Relative Power Alpha	**12**	**4** Pz, P4, Po7, Po8			**16**
Relative Power Beta	**2**	**5** F3, Fz, F4, T7, C3	**1** Fp1	**8** C4, T8, P3, Pz, P4, Po7, Po8, Oz	**16**
Total	**41**	**29**	**21**	**74**	**165**

Additionally, electrophysiological research on swallowing provides crucial insights into dysphagia. For instance, one study was conducted to evaluate dysphagia at the oropharyngeal stage of swallowing and to investigate the underlying pathophysiological mechanisms in patients with myasthenia gravis [28]. Another study explored the relationship between multiple sclerosis (MS) and dysphagia using electrophysiological methods [29]. Furthermore, research examining stroke patients and individuals with swallowing difficulties helped establish a connection between these conditions [30].

Considering these findings, we believe that EEG-based motor imagery can help identify distinct electrophysiological features, potentially advancing brain-machine interface applications for dysphagia rehabilitation. The unique neural patterns observed during motor imagery—such as imagining swallowing water versus saliva—highlight the significance of EEG-based feature extraction. These findings emphasize the crucial role of mental practice and physical therapy in motor rehabilitation, illustrating the interplay between brain activity, treatment approaches, and recovery in dysphagia patients.

Numerous studies have been conducted on the rehabilitation of swallowing disorders; however, research specifically focusing on the potential of motor imagery (MI) as a standalone approach for improving swallowing rehabilitation remains limited. Existing studies suggest that motor imagery can elicit neural responses and that mentally simulating swallowing-related actions may enhance swallowing motor performance [18].

This study used different experimental protocols to explore the relationship between motor imagery and swallowing. By examining whether motor imagery of swallowing varies across different conditions, we aimed to identify practical, cost-effective, and accessible applications that could enhance the effectiveness of active exercises in dysphagia rehabilitation. While motor imagery exercises cannot fully replace active exercises, they are recommended as a complementary approach to enhance motor learning and performance, particularly following neurological impairment. The most effective rehabilitation outcomes are achieved when physiotherapy is combined with motor imagery [31], [32], [33].

Furthermore, while previous studies have investigated various methodologies of swallow motor imagery [19], [34], [35]. They often lacked statistical analyses of the data. One of the key contributions of this study is the systematic statistical analysis of EEG signals obtained from different experimental paradigms. The results indicate that the neural responses associated with swallowing motor imagery differ significantly across experimental conditions.

In previous studies, several aspects of swallowing-related brain activity have been explored. For instance, Yang et al. demonstrated that motor imagery of swallowing activates motor-related cortical areas and suggested that gaps in brain activity may reflect the absence of swallow initiation [20], [21], [34], [36], [37], [38]. Similarly, Huckabee et al. highlighted the role of the supplementary motor area in the preparatory phase of voluntary swallowing [23].

Table 2. The mean estimates, standard errors, and corresponding channel and feature names for comparisons.

Channel	Feature name	Paradigm 1 (Mean ± STD)	Paradigm 2 (Mean ± STD)	Paradigm 3 (Mean ± STD)
CZ	theta band power	$5.22\times10^{-5} \pm 2.68\times10^{-4}$	$5.22\times10^{-5} \pm 2.68\times10^{-4}$	$5.22\times10^{-5} \pm 2.68\times10^{-4}$
CZ	alpha band power [c]	$3.28\times10^{-5} \pm 1.36\times10^{-4}$	$3.28\times10^{-5} \pm 1.36\times10^{-4}$	$3.28\times10^{-5} \pm 1.36\times10^{-4}$
CZ	relative alpha band power	0.20±0.12	0.23±0.11	0.22±0.14
CZ	relative beta band power	0.23±0.16	0.21±0.13	0.19±0.13
Fp2	theta band power	0.00±0.01	0.00±0.01	0.00±0.00
Fp3	relative alpha band power	0.19±0.12	0.20±0.11	0.19±0.13
Fp4	relative beta band power	0.22±0.16	0.19±0.13	0.17±0.13
F3	theta band power	0.04±0.16	0.02±0.07	0.02±0.06
F3	relative alpha band power	0.18±0.12	0.18±0.11	0.17±0.12
FZ	theta band power	0.29±0.84	0.16±0.34	0.19±0.34
FZ	relative alpha band power	0.18±0.12	0.16±0.11	0.16±0.12
F4	theta band power	1.16±2.71	0.69±1.09	0.84±1.33
F4	alpha band power [b]	0.53±1.11	0.30±0.27	0.50±1.45
F4	relative alpha band power	0.17±0.12	0.16±0.11	0.15±0.12
T7	theta band power	3.22±6.38	2.00±2.61	2.52±3.81
T7	alpha band power	1.41±2.30	0.87±0.78	1.40±3.61
T7	relative alpha band power	0.17±0.12	0.15±0.11	0.15±0.11
C3	theta band power	6.79±12.08	4.40±5.05	5.63±8.43
C3	alpha band power	2.94±3.79	1.95±1.76	3.04±7.40
C3	relative alpha band power	0.17±0.12	0.15±0.11	0.15±0.11
Fp1	theta band power	11.60±19.30	7.76±8.27	10.04±15.17
Fp1	alpha band power	5.07±5.39	3.57±3.27	5.46±13.07
Fp1	relative alpha band power	0.18±0.12	0.15±0.11	0.15±0.11
C4	theta band power	16.90±27.17	11.59±11.84	15.24±23.45
C4	relative alpha band power	0.18±0.12	0.15±0.11	0.15±0.11
T8	theta band power	21.88±35.10	15.33±15.34	20.20±31.74
T8	relative alpha band power	0.18±0.12	0.15±0.11	0.15±0.10
P3	theta band power [c]	25.76±42.23	18.30±18.21	24.09±38.70
P3	relative theta band power [b]	0.24±0.14	0.22±0.11	0.20±0.11
P3	relative alpha band power	0.18±0.13	0.15±0.10	0.15±0.10
PZ	theta band power	27.76±47.01	19.82±19.74	26.01±42.79
PZ	relative theta band power	0.24±0.14	0.21±0.11	0.20±0.11

Channel	Feature name	Paradigm 1 (Mean ± STD)	Paradigm 2 (Mean ± STD)	Paradigm 3 (Mean ± STD)
P4	theta band power	27.43±48.32	19.48±19.46	25.42±43.00
P4	relative theta band power	0.23±0.14	0.21±0.11	0.20±0.10
PO7	theta band power	25.02±46.90	17.39±17.46	22.61±39.66
PO7	relative theta band power	0.23±0.13	0.20±0.11	0.19±0.10
PO8	theta band power	21.50±45.68	14.13±14.33	18.92±37.49
PO8	relative theta band power	0.22±0.13	0.20±0.10	0.19±0.10
OZ	theta band power [c]	18.28±48.10	10.77±11.53	16.41±52.06
OZ	relative theta band power	0.21±0.12	0.19±0.09	0.19±0.09
OZ	relative alpha band power	0.19±0.11	0.16±0.09	0.17±0.10

a: p-value <0.05 for paradigm 1 vs. paradigm 2,

b: p-value <0.05 for paradigm 1 vs. paradigm 3,

c: p-value <0.05 for paradigm 2 vs. paradigm 3.

Table 3. Classification accuracies (%) of different classifier paradigms for various class combinations using 135 significant features.

Classifier/Paradigm	**1 vs 2**	**2 vs 3**	**1 vs 3**	**1 vs 2 vs 3**
Random Forest	75.26%	71.58%	76.58%	60.18%
SVM (RBF)	70.79%	63.95%	70.00%	51.40%
KNN	69.21%	62.37%	68.16%	51.75%
Decision Tree	74.74%	70.26%	77.11%	59.47%

Our findings are consistent with these observations, as we also identified significant differences in spectral centroid and frequency band powers during the imagination of swallowing under different conditions, reflecting distinct cortical engagement.

Jestrovic et al. reported that attentional modulation can influence EEG activity during swallowing tasks, indicating that task design may affect cortical activation patterns [22]. In our study, the use of visual cues for imagination phases (in induced saliva and induced water paradigms) allowed us to observe more temporally controlled cortical responses compared to the natural swallowing condition, where imagination onset was more spontaneous.

Furthermore, previous studies, such as those by Kober et al., primarily used hemodynamic measurements (e.g., NIRS) or did not provide detailed statistical analyses of motor imagery EEG data [39]. In contrast, our study employed comprehensive frequency-domain feature extraction combined with statistical evaluation (ANOVA and Friedman tests), which revealed that 76.7% of features exhibited significant differences across conditions. This systematic analysis contributes novel insights into the electrophysiological characterization of swallowing motor imagery and supports the feasibility of using EEG-based biomarkers for dysphagia rehabilitation.

As a novel approach to swallowing rehabilitation, this study was conducted on healthy individuals. We chose this approach based on the rationale that an initial focus on healthy participants would provide a clearer understanding of the natural swallowing process before extending the research to individuals with dysphagia. Including individuals with swallowing disorders at this stage could introduce confounding factors that might obscure the fundamental characteristics of motor imagery-related neural activity.

Overall, the findings of this study contribute to the growing body of knowledge on dysphagia rehabilitation and provide a foundation for developing more effective motor imagery-based therapeutic strategies. This research offers promising insights that may help optimize dysphagia rehabilitation programs and improve educational approaches for both clinicians and patients.

The primary limitation of this study was the variability in the timing of motor imagery across individuals. As a result, we had to analyze each trial separately, which made it challenging to establish a generalized structure with high external validity. Additionally, since the act of swallowing introduces significant noise in EEG signals, denoising the data proved to be a major challenge. However, the statistical analyses performed in this study have contributed to a better understanding of the neural mechanisms underlying the swallowing process. One limitation of the natural water swallowing paradigm was the absence of externally

provided cues for motor imagery onset, which may introduce subjective variability in determining the imagination periods. Although segment selection was based on visual inspection of muscle artifacts to identify pre-swallowing periods, potential inter-observer variability may affect the consistency of these segments.

For future studies, we aim to further improve the distinction between swallowing, rest, and imagination states by employing advanced classification methods. Moreover, we plan to expand our experimental design by incorporating additional experimental paradigms that allow for a clearer comparison between different conditions. Another crucial direction for future research is to extend this work to individuals with dysphagia, allowing for a comparative analysis between healthy participants and patients. This will provide a deeper insight into the motor imagery of swallowing and its potential applications in rehabilitation. Additionally, in future studies, we would like to use additional objective measurements such as electromyography (EMG) or laryngeal sensors to more accurately detect pre-swallow onset during natural swallowing paradigms.

Additionally, we intend to develop a novel brain-machine interface (BMI) based EEG decoding approach specifically tailored for dysphagia patients. Such advancements may facilitate the creation of more effective motor imagery-based rehabilitation strategies, ultimately improving therapeutic outcomes for individuals with swallowing disorders.

Funding Statement: The authors received no financial support for the research, authorship, and/or publication of this article.

Conflict of Interest Statement: The authors declare no conflict of interest.

Ethical Statement: The Declaration of Helsinki conducted all study procedures. This study was approved by the Erciyes University Ethics Committee on July 12, 2023, under approval number 2023/461.

References

[1] D. G. Smithard, P. A. O'Neill, R. E. England, C. L. Park, R. Wyatt, D. F. Martin, and J. Morris, "Complications and outcome after acute stroke: Does dysphagia matter?," Stroke, vol. 27, no. 7, pp. 1200–1204, 1996, doi: 10.1161/01.STR.27.7.1200.

[2] J. M. Dudik, A. Kurosu, J. L. Coyle, and E. Sejdić, "Dysphagia and its effects on swallowing sounds and vibrations in adults," Biomed. Eng. Online, vol. 17, no. 1, 2018, doi: 10.1186/s12938-018-0501-9.

[3] P. M. Bath, H. S. Lee, and L. F. Everton, "Swallowing therapy for dysphagia in acute and subacute stroke," Stroke, 2019, doi: 10.1161/STROKEAHA.118.024299.

[4] P. Leslie, M. J. Drinnan, I. Zammit-Maempel, J. L. Coyle, G. A. Ford, and J. A. Wilson, "Cervical auscultation synchronized with images from endoscopy swallow evaluations," Dysphagia, vol. 22, no. 4, pp. 290–298, 2007, doi: 10.1007/s00455-007-9084-5.

[5] S. E. Langmore, "Evaluation of oropharyngeal dysphagia: Which diagnostic tool is superior?," Curr. Opin. Otolaryngol. Head Neck Surg., vol. 11, no. 6, pp. 485–489, 2003, doi: 10.1097/00020840-200312000-00014.

[6] J. L. Coyle et al., "Oropharyngeal dysphagia assessment and treatment efficacy: Setting the record straight (Response to Campbell-Taylor)," J. Am. Med. Dir. Assoc., vol. 10, no. 1, pp. 62–66, 2009, doi: 10.1016/j.jamda.2008.10.003.

[7] C. D. Binnie and P. F. Prior, "Electroencephalography," J. Neurol. Neurosurg. Psychiatry, vol. 57, no. 11, pp. 1308–1319, 1994, doi: 10.1136/jnnp.57.11.1308.

[8] M. Proudfoot, M. W. Woolrich, A. C. Nobre, and M. R. Turner, "Magnetoencephalography," Pract. Neurol., vol. 14, no. 5, pp. 336–343, 2014, doi: 10.1136/practneurol-2013-000768.

[9] G. Muehllehner and J. S. Karp, "Positron emission tomography," Phys. Med. Biol., vol. 51, no. 13, pp. R117–R137, 2006, doi: 10.1088/0031-9155/51/13/R08.

[10] G. Niso, E. Romero, J. T. Moreau, A. Araujo, and L. R. Krol, "Wireless EEG: A survey of systems and studies," Neuroimage, vol. 269, 2023, Art. no. 119774, doi: 10.1016/j.neuroimage.2022.119774.

[11] C. Yen, C. L. Lin, and M. C. Chiang, "Exploring the frontiers of neuroimaging: A review of recent advances in understanding brain functioning and disorders," Life, vol. 13, no. 7, p. 1472, 2023, doi: 10.3390/life13071472.

[12] H. Namazi, E. Aghasian, and T. S. Ala, "Fractal-based classification of electroencephalography (EEG) signals in healthy adolescents and adolescents with symptoms of schizophrenia," Technol. Health Care, vol. 27, no. 3, pp. 231–242, 2019, doi: 10.3233/THC-181497.

[13] J. Chouinard, "Dysphagia in Alzheimer disease: A review," J. Nutr. Health Aging, vol. 4, no. 4, pp. 214–217, 2000.

[14] H. Azuma and T. Akechi, "EEG correlates of quality of life and associations with seizure without awareness and depression in patients with epilepsy," Neuropsychopharmacol. Rep., vol. 42, no. 3, pp. 281–289, 2022, doi: 10.1002/npr2.12276.

[15] Ö. Türk and M. S. Özerdem, "Epilepsy detection by using scalogram based convolutional neural network from EEG signals," Brain Sci., vol. 9, no. 5, p. 115, 2019, doi: 10.3390/brainsci9050115.

[16] S. Abenna, M. Nahid, H. Bouyghf, and B. Ouacha, "An enhanced motor imagery EEG signals prediction system in real-time based on delta rhythm," Biomed. Signal Process. Control, vol. 79, 2023, Art. no. 104210, doi: 10.1016/j.bspc.2022.104210.

[17] A. Al-Saegh, S. A. Dawwd, and J. M. Abdul-Jabbar, "Deep learning for motor imagery EEG-based classification: A review," Biomed. Signal Process. Control, vol. 63, p. 102172, 2021, doi: 10.1016/j.bspc.2020.102172.

[18] A. S. C. Caldas et al., "Motor imagery and swallowing: a systematic literature review," Rev. CEFAC, vol. 20, no. 2,

pp. 249–258, 2018, doi: 10.1590/1982-0216201820214317.

[19] S. SH, N. CV, and D. CRO, "Motor imagery and swallowing: Introduction to literature and discussion of research needs in dysphagia," Health Care Curr. Rev., vol. 6, no. 1, 2018, doi: 10.4172/2375-4273.1000218.

[20] H. Yang et al., "Detection of motor imagery of swallow with model adaptation: Swallow or tongue?," in Proc. 5th Int. Brain-Computer Interface Meeting, 2013, doi: 10.3217/978-3-85125-260-6-56.

[21] H. Yang et al., "On the correlations of motor imagery of swallow with motor imagery of tongue movements and actual swallow," in Proc. Int. Conf. Neural Inf. Process., 2016, pp. 481–488, doi: 10.1007/978-981-10-0207-6_55.

[22] I. Jestrović, J. L. Coyle, S. Perera, and E. Sejdić, "Influence of attention and bolus volume on brain organization during swallowing," Brain Struct. Funct., vol. 223, no. 2, pp. 749–761, 2018, doi: 10.1007/s00429-017-1535-7.

[23] M. L. Huckabee, L. Deecke, M. P. Cannito, H. J. Gould, and W. Mayr, "Cortical control mechanisms in volitional swallowing: The Bereitschaftspotential," Brain Topogr., vol. 16, no. 1, pp. 3–17, 2003, doi: 10.1023/A:1025671914949.

[24] A. Alexandropoulou, E. Magkouti, A. Despoti, N. Leventakis, and S. Nanas, "Studying the swallow using surface electroencephalography: A systematic review," Health Res. J., vol. 9, no. 2, pp. 63–75, 2023, doi: 10.12681/healthresj.33617.

[25] N. M. Y. B. W. Razali, "Power comparison of Shapiro-Wilk, Kolmogorov-Smirnov, Lilliefors, and Anderson-Darling tests," J. Stat. Model. Anal., vol. 2, no. 1, pp. 21–33, 2011.

[26] I. Jestrović, J. L. Coyle, and E. Sejdić, "Decoding human swallowing via electroencephalography: A state-of-the-art review," J. Neural Eng., vol. 12, no. 5, p. 051001, 2015, doi: 10.1088/1741-2560/12/5/051001.

[27] S. McWeeny and E. S. Norton, "Understanding event-related potentials (ERPs) in clinical and basic language and communication disorders research: A tutorial," Int. J. Lang. Commun. Disord., vol. 55, no. 5, pp. 649–663, 2020, doi: 10.1111/1460-6984.12535.

[28] C. Ertekin, N. Yüceyar, and I. Aydoğdu, "Clinical and electrophysiological evaluation of dysphagia in myasthenia gravis," J. Neurol. Neurosurg. Psychiatry, vol. 65, no. 6, pp. 848–856, 1998, doi: 10.1136/jnnp.65.6.848.

[29] Y. Beckmann et al., "Electrophysiological evaluation of dysphagia in the mild or moderate patients with multiple sclerosis: A concept of subclinical dysphagia," Dysphagia, vol. 30, no. 3, pp. 331–338, 2015, doi: 10.1007/s00455-015-9598-1.

[30] B. Labeit et al., "The assessment of dysphagia after stroke: State of the art and future directions," Lancet Neurol., vol. 22, no. 7, pp. 590–600, 2023, doi: 10.1016/S1474-4422(23)00153-9.

[31] C. G. Ashley Fox, "Using motor imagery therapy to improve movement efficiency and reduce fall injury risk," J. Nov. Physiother., vol. 3, no. 6, p. 186, 2013, doi: 10.4172/2165-7025.1000186.

[32] T. Singer, P. Fahey, and K. P. Y. Liu, "The efficacy of imagery in the rehabilitation of people with Parkinson's disease: Protocol for a systematic review and meta-analysis," Syst. Rev., vol. 11, no. 1, p. 47, 2022, doi: 10.1186/s13643-022-02041-z.

[33] A. M. Ladda, F. Lebon, and M. Lotze, "Using motor imagery practice for improving motor performance – A review," Brain Cogn., vol. 150, p. 105705, 2021, doi: 10.1016/j.bandc.2021.105705.

[34] H. Yang et al., "Detection of motor imagery of swallow EEG signals based on the dual-tree complex wavelet transform and adaptive model selection," J. Neural Eng., vol. 11, no. 3, p. 035016, 2014, doi: 10.1088/1741-2560/11/3/035016.

[35] S. E. Kober and G. Wood, "Changes in hemodynamic signals accompanying motor imagery and motor execution of swallowing: A near-infrared spectroscopy study," Neuroimage, vol. 93, no. Pt 1, pp. 1–10, 2014, doi: 10.1016/j.neuroimage.2014.02.019.

[36] H. Yang, K. K. Ang, C. Wang, K. S. Phua, and C. Guan, "Neural and cortical analysis of swallowing and detection of motor imagery of swallow for dysphagia rehabilitation—A review," in Prog. Brain Res., vol. 228, pp. 271–295, 2016, doi: 10.1016/bs.pbr.2016.03.014.

[37] H. Yang, C. Guan, K. K. Ang, C. C. Wang, K. S. Phua, and J. Yu, "Dynamic initiation and dual-tree complex wavelet feature-based classification of motor imagery of swallow EEG signals," in Proc. Int. Joint Conf. Neural Netw. (IJCNN), 2012, pp. 1–7, doi: 10.1109/IJCNN.2012.6252603.

[38] H. Yang et al., "Feature consistency-based model adaptation in session-to-session classification: A study using motor imagery of swallow EEG signals," in Proc. Annu. Int. Conf. IEEE Eng. Med. Biol. Soc. (EMBC), 2013, pp. 5438–5441, doi: 10.1109/EMBC.2013.6609528.

[39] S. E. Kober, D. Grössinger, and G. Wood, "Effects of motor imagery and visual neurofeedback on activation in the swallowing network: A real-time fMRI study," Dysphagia, vol. 34, no. 6, pp. 763–775, 2019, doi: 10.1007/s00455-019-09985-w.